



Aggregated and Hyperstable Damage-Associated Molecular Patterns Are Released During ER Stress to Modulate Immune Function

Alexander Andersohn^{1†}, M. Iveth Garcia^{1†}, Ying Fan^{1†}, Max C. Thompson¹, Askar M. Akimzhanov¹, Abdikarim Abdullahi², Marc G. Jeschke^{2*} and Darren Boehning^{1,3*}

¹ Department of Biochemistry and Molecular Biology, McGovern Medical School at UTHealth, Houston, TX, United States,

² Ross Tilley Burn Centre, Sunnybrook Health Sciences Centre, Toronto, ON, Canada, ³ Department of Biomedical Sciences, Cooper Medical School of Rowan University, Camden, NJ, United States

OPEN ACCESS

Edited by:

Ashok Kumar,
University of Houston, United States

Reviewed by:

Alok Chandra Bharti,
University of Delhi, India
Arion Kennedy,
North Carolina State University,
United States

*Correspondence:

Marc G. Jeschke
Marc.Jeschke@sunnybrook.ca
Darren Boehning
boehning@rowan.edu

[†] These authors have contributed
equally to this work

Specialty section:

This article was submitted to
Molecular Medicine,
a section of the journal
Frontiers in Cell and Developmental
Biology

Received: 24 May 2019

Accepted: 02 September 2019

Published: 18 September 2019

Citation:

Andersohn A, Garcia MI, Fan Y, Thompson MC, Akimzhanov AM, Abdullahi A, Jeschke MG and Boehning D (2019) Aggregated and Hyperstable Damage-Associated Molecular Patterns Are Released During ER Stress to Modulate Immune Function. *Front. Cell Dev. Biol.* 7:198. doi: 10.3389/fcell.2019.00198

Chronic ER stress occurs when protein misfolding in the Endoplasmic reticulum (ER) lumen remains unresolved despite activation of the unfolded protein response. We have shown that traumatic injury such as a severe burn leads to chronic ER stress *in vivo* leading to systemic inflammation which can last for more than a year. The mechanisms linking chronic ER stress to systemic inflammatory responses are not clear. Here we show that induction of chronic ER stress leads to the release of known and novel damage-associated molecular patterns (DAMPs). The secreted DAMPs are aggregated and markedly protease resistant. ER stress-derived DAMPs activate dendritic cells (DCs) which are then capable of polarizing naïve T cells. Our findings indicate that induction of chronic ER stress may lead to the release of hyperstable DAMPs into the circulation resulting in persistent systemic inflammation and adverse outcomes.

Keywords: ER stress, damage-associated molecular pattern, DAMP, cytokine, dendritic cell, inflammation, trauma, burn

INTRODUCTION

The endoplasmic reticulum (ER) is the site of secretory and membrane-bound protein synthesis. Under conditions where ER protein synthesis rates exceed the folding capacity of the ER, unfolded or misfolded proteins accumulate in the ER lumen or membrane. The presence of an excess of misfolded proteins in the ER results in the activation of ER stress signaling pathways to restore homeostasis (Almanza et al., 2019). For example, ER chaperone content is increased while global protein synthesis rates are decreased in an effort to resolve the folding stress. If ER luminal protein folding stress cannot be resolved, pro-apoptotic pathways are activated resulting in cell death (Sano and Reed, 2013; Sovolyova et al., 2014). Chronic ER stress is characterized by activation of this pathway without significant cell death resulting in cellular and organ dysfunction over extended time periods (Oakes and Papa, 2015). Inflammatory stimuli can lead to chronic ER stress in multiple cells and tissues (Hotamisligil, 2010). For example, activation of the acute phase response results in dramatic upregulation in the synthesis of secretory proteins such as C-reactive protein resulting in hepatic ER stress (Zhang et al., 2006; Alicka and Marycz, 2018). We previously found that chronic ER stress is prominent post-burn injury and persists for an extended period after the initial insult

(Gauglitz et al., 2009, 2010; Jeschke et al., 2009, 2012; Song et al., 2009, 2012; Jeschke and Boehning, 2011, 2012; Brooks et al., 2013; Diao et al., 2014). How chronic ER stress mechanistically contributes to post-burn inflammation and metabolic dysfunction is still unclear.

NLR Family Pyrin Domain Containing 3 (NLRP3) plays a central role in regulating inflammatory signaling transmitted by damage-associated molecular pattern molecules (DAMPs) derived from stressed or damaged cells (He et al., 2016; Jo et al., 2016). Inflammatory DAMPs include intracellular proteins such as high mobility group box 1 (HMGB1) and non-protein DAMPs such as nucleic acids, both of which are released from dying/damaged cells. Inflammasome activation by DAMPs leads to caspase 1 activation, resulting in maturation and secretion of IL-1 β and downstream inflammatory responses (Choi and Nakahira, 2011; Davis et al., 2011). DAMP molecules are known to significantly contribute to systemic inflammation and adverse outcomes in trauma (Tang et al., 2012; Rani et al., 2017). We have previously shown that NLRP3 activation is central to post-burn responses including the induction of ER stress and systemic inflammation (Diao et al., 2014; Stanojic et al., 2014; Vainik et al., 2018). Pro-inflammatory cytokines such as IL-6 and IL-1 β can lead to ER stress highlighting a positive feedback loop promoting inflammatory signaling (O'Neill et al., 2013; Liu et al., 2015; Carta et al., 2017). Thus, DAMPs may contribute to systemic inflammation and long-lasting metabolic dysfunction after burn injury.

Endoplasmic reticulum stress is known to induce the release of DAMPs. For example, chemotherapeutics can induce ER stress leading to the release of DAMPs and “immunogenic cell death” of cancer cells (van Vliet et al., 2015; Rufo et al., 2017). It has also been shown that ER stress can lead to the release of DAMPs within secreted extracellular vesicles (Collett et al., 2018). Here we show that inducing chronic ER stress in hepatoma cells leads to the release of non-vesicular DAMPs that are aggregated and hyperstable as determined by protease sensitivity. DAMP release was most likely associated with amphisome-mediated secretion *versus* apoptotic/necrotic cell permeabilization. The released DAMPs potentially stimulated dendritic cell activation and the production of inflammatory mediators. Our results provide a mechanistic link between chronic ER stress with the long-lasting inflammation and hypermetabolism found in trauma patients with significant therapeutic implications.

RESULTS

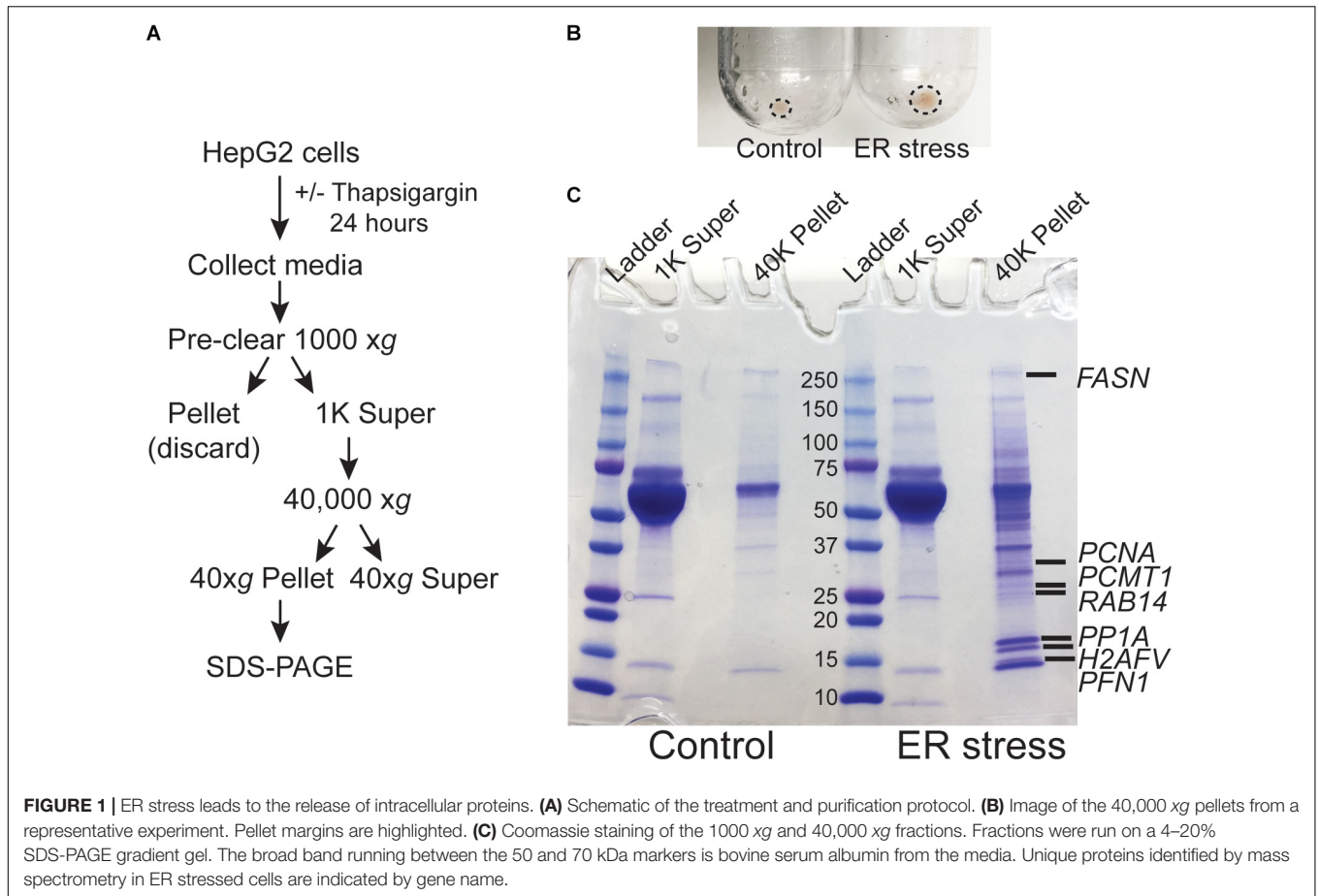
ER Stress Leads to the Secretion of Intracellular Proteins Into the Extracellular Space

We previously demonstrated that ER calcium store depletion is a central mediator of post-burn hepatic ER stress (Jeschke et al., 2009). To model this *in vitro* we depleted ER calcium stores with the SERCA pump inhibitor thapsigargin (TG) in HepG2 hepatoma cells, a well-characterized polarized human hepatocyte cell line model (Slany et al., 2010; Qiu et al., 2015).

We hypothesized that ER stress may lead to the release of aggregated proteins and/or extracellular vesicles into the media which could function as DAMPs. HepG2 cells were treated with TG for 24 h and the media was subjected to differential centrifugation as in **Figure 1A**. There was a notable increase in the size of the cell-free high speed pellet in cells subjected to ER stress (**Figure 1B**). When the 40,000 g supernatant and pellet fractions were run on SDS-PAGE, a large number of additional proteins were apparent in the pellet fraction of ER-stressed cells (**Figure 1C**). Identification of the bands by mass spectrometry analysis revealed established DAMPs, such as histones, among other proteins which have not yet been established as *bone fide* DAMPs (**Supplementary Dataset S1**).

Protein Released During ER Stress Are Non-vesicular and Protease Resistant

Recent evidence indicates that DAMPs may be secreted as extracellular vesicles during ER stress (Caruso and Poon, 2018; Collett et al., 2018). To test whether the secreted proteins identified in **Figure 1** are present within lipid vesicles, we subjected the 40,000 g pellet to an additional purification step through a sucrose cushion. Using this protocol, vesicular components should remain in the sucrose cushion whereas high molecular weight non-vesicular (NV) components such as aggregated proteins will pellet through the cushion (**Figure 2A**; Faruqi et al., 2018; Gupta et al., 2018; Konoshenko et al., 2018). Using this fractionation protocol, there was a large prominent pellet present only in ER stressed cells (**Figure 2B**). When run on SDS-PAGE followed by Coomassie staining, the pellet fraction from ER stressed cells had an abundant number of proteins, some of which were also prominent in the 40,000 g fraction (**Figure 2C** and **Supplementary Dataset S2**). Similar results were found in cells treated for 48 h with TG (**Supplementary Figure S1**). Many of the proteins found in the 100,000 g fraction were also isolated in the NV fraction from another recent study which provided evidence that they are secreted in an amphisome-dependent manner [(Jeppesen et al., 2019); **Supplementary Dataset S1**]. Dilution of the sucrose cushion fraction and re-centrifugation to isolate extracellular vesicles resulted in no detectable protein by the Bradford method (Bradford, 1976). Similarly, running the extracellular vesicle fraction on SDS-PAGE resulted in no visible protein by Coomassie staining, indicating that extracellular vesicles are secreted at undetectable levels in HepG2 cells under the specific conditions used in this study. We will use the NV fraction for the remainder of this study since ER stress induced a dramatic upregulation of the proteins isolated from this fraction. Some of the proteins secreted from ER stressed cells are established DAMPs, such as histones, actin, and HMGB1 (**Figure 2C**; highlighted in bold). Western blotting confirmed the presence of these proteins in the NV fraction derived from the media of ER stressed cells (**Figure 2D**). We confirmed by Western blotting the presence of several other proteins which are not classically characterized as DAMPs such as profilin-1 and enolase-1 (**Figure 2D**). ER stress leads to the production of misfolded and aggregated proteins which would be predicted to have increased resistance to protease



digestion. To test whether proteins derived from the NV fractions were aggregated, we subjected these fractions to limited trypsin digestion. As a control we utilized total protein HepG2 Triton-X100 lysates. As shown in **Figure 2E**, almost all proteins present in HepG2 Triton-X100 lysates were digested within 15 min by *in vitro* trypsin digestion (**Figure 2E**). In sharp contrast, most proteins in the NV preps from ER stressed cells were detectable for the entire 180 min time course (**Figure 2F**). Thus, ER stress leads to the secretion of known, and potentially novel, highly protease-resistant DAMPs which are not present within extracellular vesicles.

Activation of Apoptotic/Necroptotic Programs During ER Stress

Release of NV proteins may either be through lysis of the plasma membrane or regulated release through other mechanisms such as the classical secretory pathway or non-canonical pathways such as the release of amphisome contents after fusion with the plasma membrane. It is thus important to discriminate whether NV protein release is due to ER stress-induced cell death or secretory mechanisms. To test these possibilities, we examined the activation of apoptotic and necrotic pathways in ER stressed HepG2 cells (**Figure 3A**). Thapsigargin dose-dependently induced the expression of BiP at all concentrations

of TG after 24 h of treatment, indicating potent activation of the ER stress program (**Figure 3B**). The broad spectrum kinase inhibitor staurosporine (STS), a positive control for the induction of apoptosis, did not induce BiP expression as expected (**Figure 3B**). Light microscopy revealed visible cell loss only at TG concentration higher than 1 μ M (**Supplementary Figure S2**). Consistent with this observation, significant cleavage of the caspase and calpain substrate α -fodrin was only obvious at TG concentrations of 1 μ M and above (**Figure 3C**). To more quantitatively assess apoptosis induction, we measured enzymatic caspase-3 activities in lysates from HepG2 cells treated with either TG or STS. Concentrations of TG between 100 nM and 10 μ M significantly activated caspase-3, however, at much lower levels than the classic apoptosis inducer STS (**Figure 3D**). Propidium iodide (PI) is a cell-impermeant DNA dye commonly used to evaluate cell membrane permeabilization in apoptotic/necrotic models. Surprisingly, the number of PI positive cells in TG treated cells was higher than in STS treated cells at all concentrations except 10 nM (**Figure 3E**). One possible interpretation is that TG activated necroptotic signaling resulting in membrane permeabilization. However, there was no evidence of necroptosis activation as determined by phospho-MLKL (Ser358) Western blotting (**Figures 3F–I**). Single cell imaging of PI stained cells revealed TG treated cells did not display canonical nuclear staining, but rather

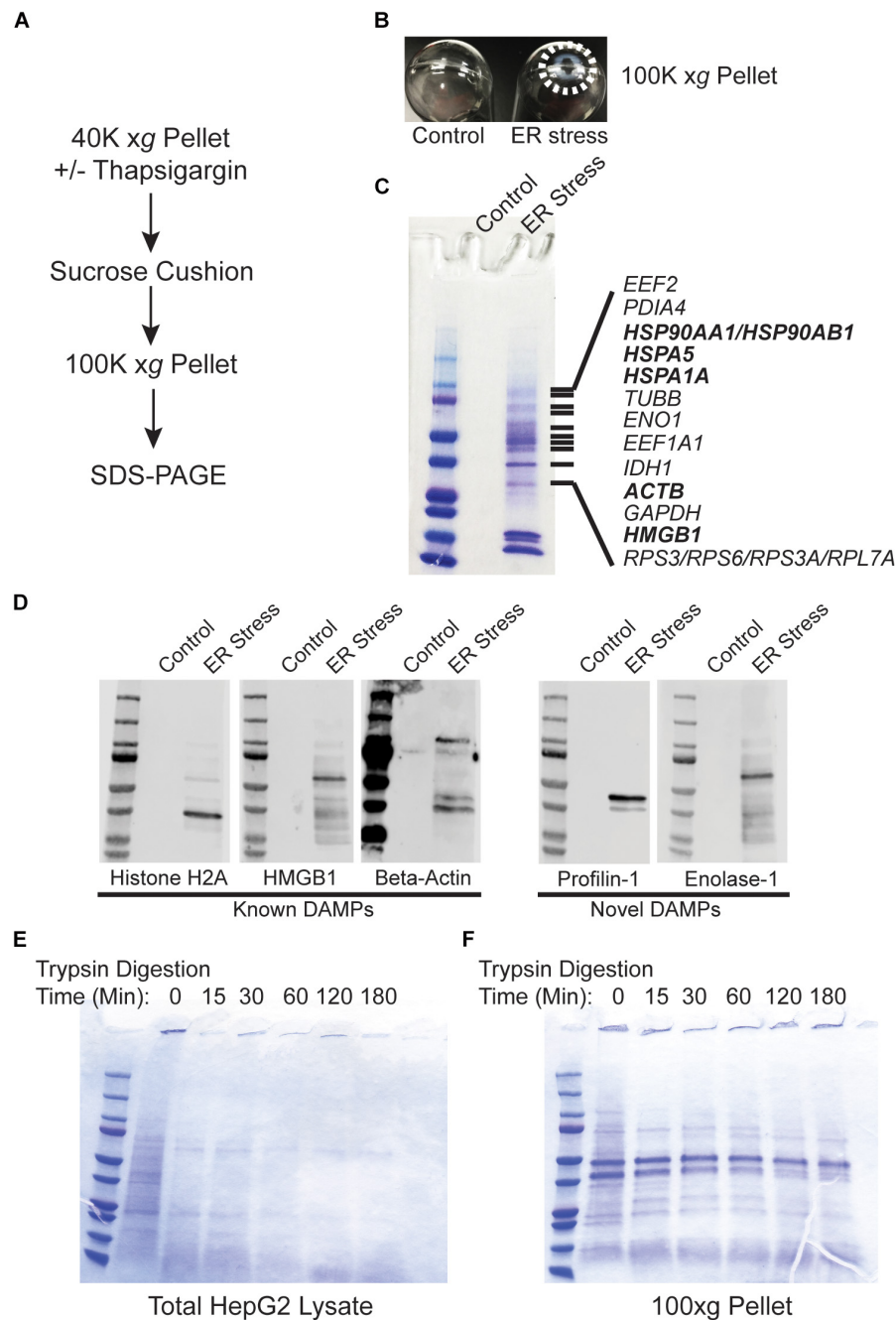
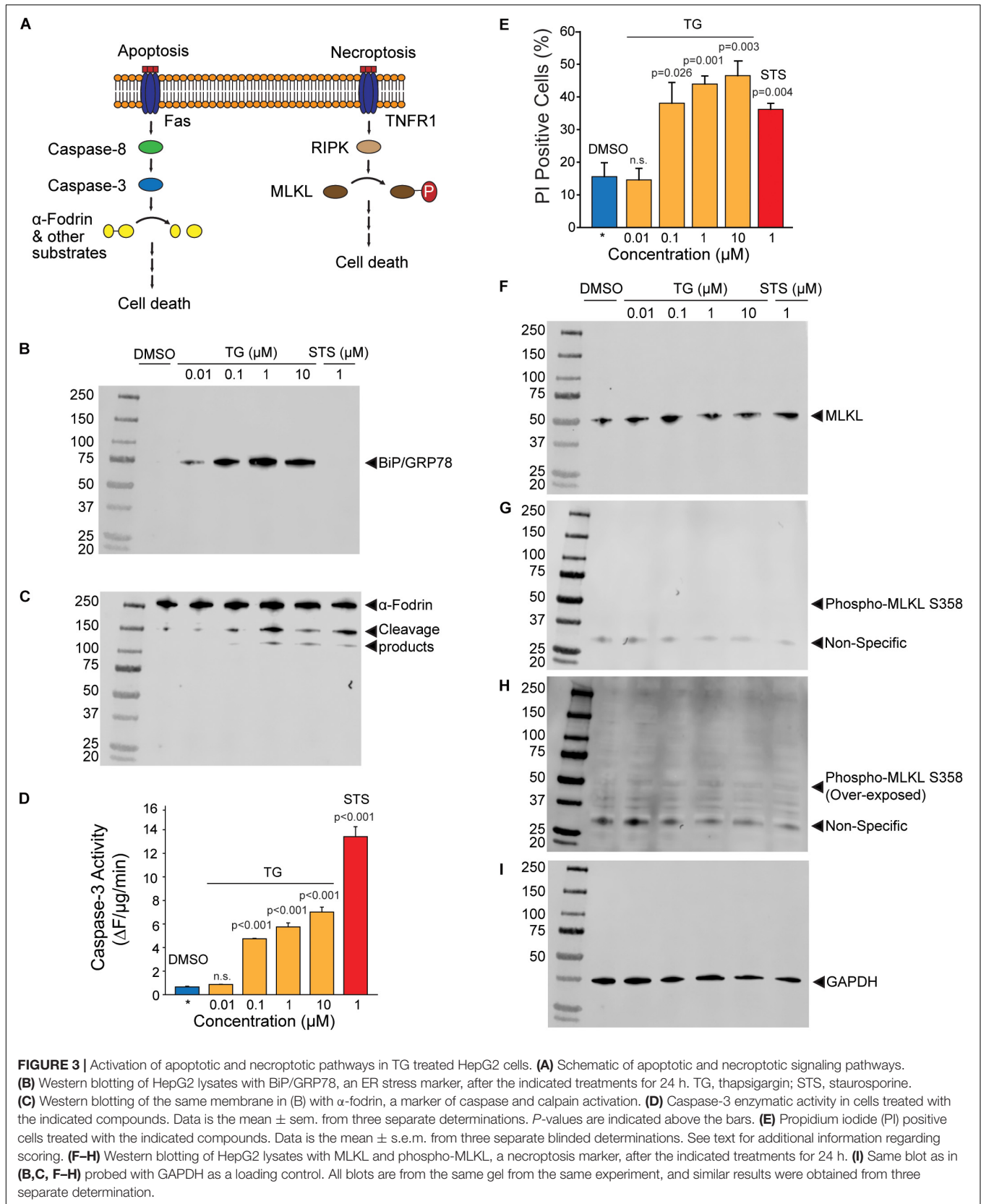
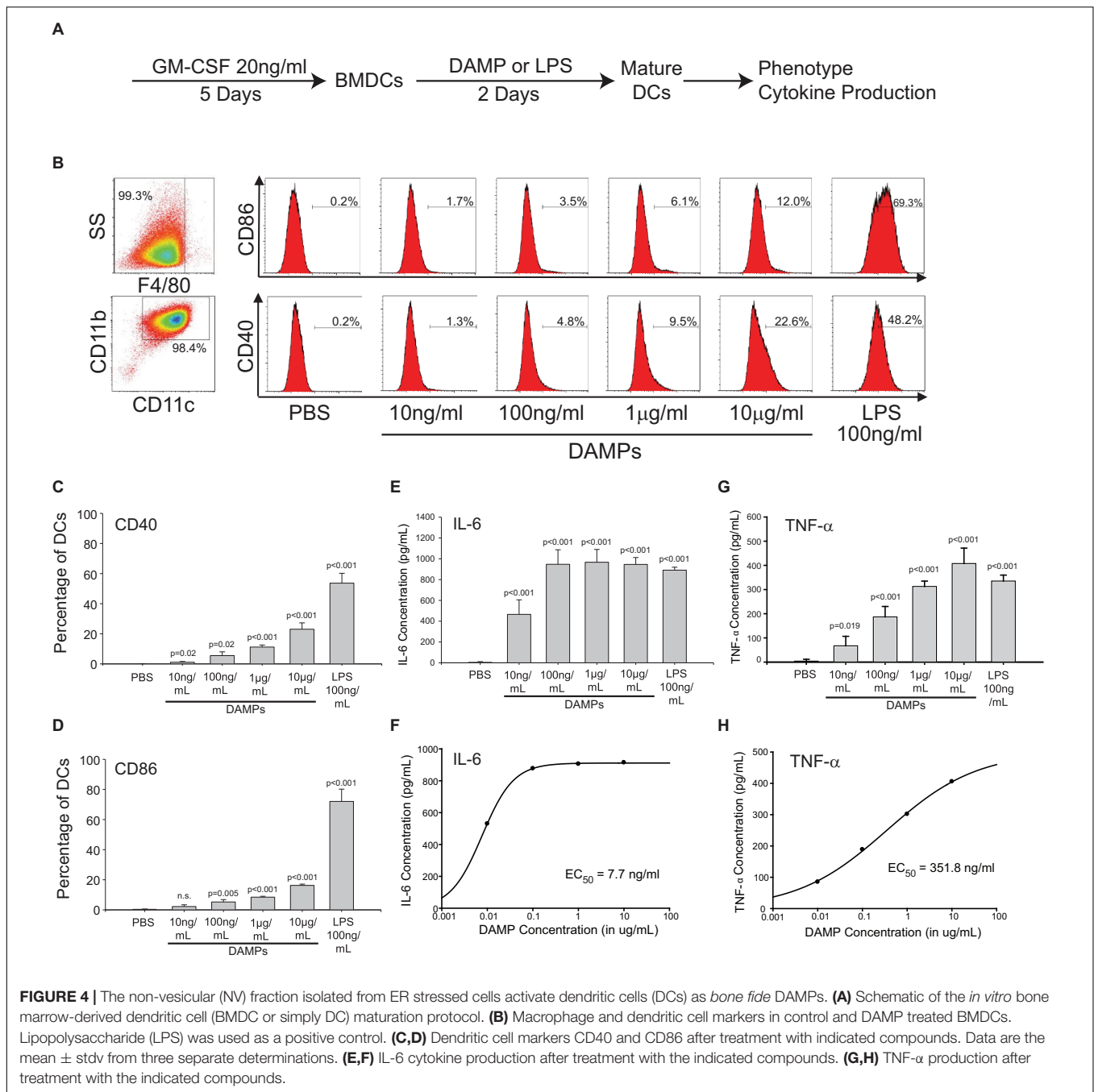


FIGURE 2 | Proteins released from ER stressed cells are non-vesicular and protease resistant. **(A)** Schematic of the purification scheme. **(B)** Image of the 100,000 xg pellets from a representative experiment. Pellet margins are highlighted. Control (DMSO) treated cells do not have a visible pellet. **(C)** Unique proteins identified by mass spectrometry in ER stressed cells are indicated by gene name. Known DAMPs are indicated in bold. **(D)** SDS-PAGE and Western blotting of a preparation as in **(C)** and identification with antibodies to the indicated proteins. **(E)** Trypsin digestion of HepG2 total cell lysate for the indicated times followed by Coomassie staining. **(F)** Trypsin digestion of the 100,000 xg pellet isolated from the media of ER stressed cells for the indicated times followed by Coomassie staining.

showed peripherally associated DNA staining (**Supplementary Figure S3**). We interpret this finding to indicate the amphisome-mediated secretion of free nucleic acids as seen by others (Jeppesen et al., 2019) which are then stained by extracellular propidium iodide. Future work will be needed to confirm

this interpretation. Regardless, it is possible to readily purify biochemically characterizable NV fractions from less than 100 ml of media of HepG2 cells treated with doses of TG as low as 100 nM. This concentration of TG leads to minimal activation of apoptotic/necroptotic signaling pathways,





indicating a primarily secretion-based mechanism for NV protein release.

ER Stress-Derived DAMPs Regulate the Expression of Costimulatory Molecules and Cytokine Production in Dendritic Cells

The NV fractions purified from ER stressed HepG2 cells contain well-characterized DAMPs (Figures 1, 2). To test whether the NV fraction from ER stressed cells functions as a *bone fide*

immune modulator, we tested whether this fraction could dose-dependently promote the maturation and activation of dendritic cells (DCs) (Fang et al., 2014). During the development from bone marrow derived monocytes to DCs, there is a loss of macrophage marker F4/80 and increased expression of CD11b and CD11c (Figures 4A,B; Wang et al., 2016). To determine whether the putative NV-derived DAMPs shape DC phenotypes, we stimulated immature DCs with increasing concentrations of DAMPs purified from HepG2 cells treated with 100 nM TG. As a positive control we utilized 100 ng/mL lipopolysaccharide (LPS) and as a negative control we utilized PBS (vehicle).

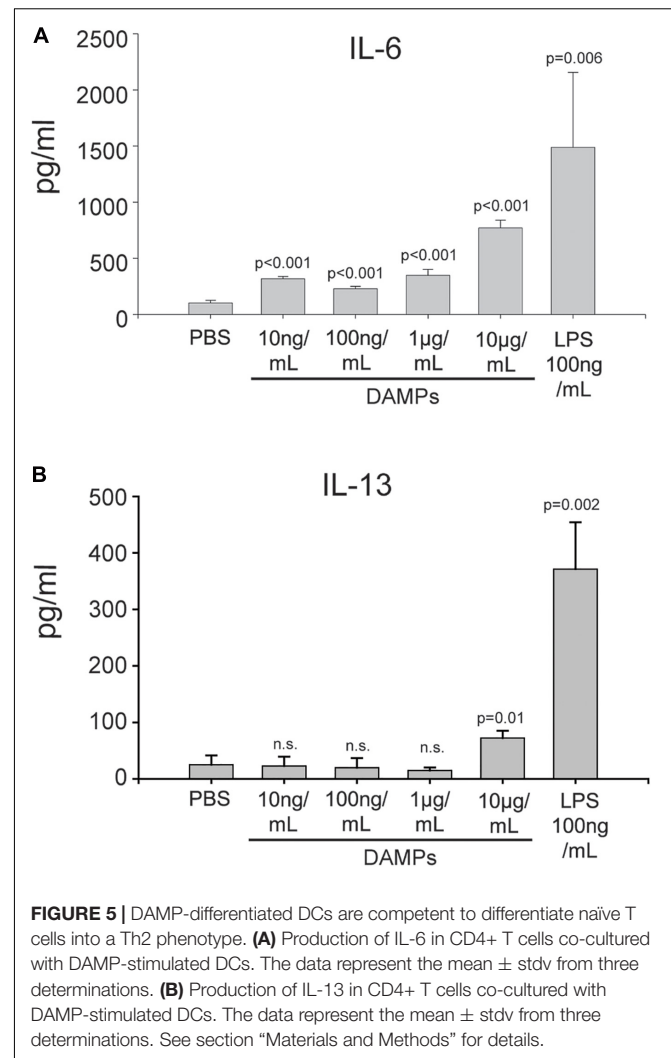
About 50% of DAMP-treated DCs were MHCII+, a marker suggesting they were ready to present antigens (**Supplementary Figure S4**). As shown in **Figure 4B**, DCs had increased expression of activation marker CD40 and CD86 as a function of DAMP concentration. Vehicle (PBS) treated DCs had no expression of CD40 or CD86. LPS is a well-known activator of DCs through TLR4. LPS treated DCs had strong expression of both CD40 and CD86. We next examined cytokine production in DAMP treated DCs. Both IL-6 and TNF- α production increased corresponding to DAMP concentration but in different manners. IL-6 production reached a plateau around 1 ng/mL when treated with 100 ng/mL DAMP. In contrast, TNF- α production kept rising as DAMP concentration was increased (**Figures 4E–H**). Although LPS induced stronger expression of CD40 and CD86, DAMP treatment induced similar levels of cytokine production when compared to LPS. These data demonstrate that the NV fraction purified from ER stressed HepG2 cells functions as a potent DAMP leading to the maturation of DCs and cytokine production.

Dendritic Cells Matured by NV-Derived DAMPs Polarize Naïve CD4+ T Cells Into a Th2/Treg Phenotype

Maturation of DCs through danger signals can be translated into the promotion of an inflammatory T-cell response. To further evaluate how NV-derived DAMPs modulate immune responses, DAMP-matured DCs were co-cultured with naïve CD4+ murine T cells for 5 days without additional DAMP stimulation. DAMP and LPS-matured DCs were both capable of stimulating T cell proliferation and activation (**Supplementary Figures S5, S6**). The DC/T cell co-culture supernatants were collected for cytokine analysis. After co-culture with DAMP-matured DCs, naïve CD4+ T cells produced a high amount of the Th2 cytokine IL-6 in a dose-dependent manner (**Figure 5A**). Moderate amounts of the Th2 cytokine IL-4 was present in all conditions (**Supplementary Figure S7**). However, even DCs treated with a relatively high concentration of DAMPs (10 μ g/mL) could not induce T cells to produce another Th2 cytokine, IL-13 (**Figure 5B**). We also tested cytokines of other T helper cell phenotypes, however, very little INF- γ and no IL-17 production was detectable suggesting that the T cells were only differentiated into the Th2 phenotype (**Supplementary Figure S7**). Finally, the Treg marker IL-10 was induced by all concentrations of DAMPs (**Supplementary Figure S7**). Thus, DCs were competent to present NV-derived DAMPs as a pro-inflammatory signal to T cells and could successfully induce a Th2 reaction. However, anti-inflammatory Treg reactions were also induced as evidenced by the production of IL-10. These findings have significant implications for systemic inflammatory responses in diseases associated with ER stress such as diabetes, cardiovascular disease, and trauma.

DISCUSSION

In this report we show that inducing low levels of ER stress in HepG2 cells leads to the release of DAMPs in the context



of minimal cell death. In our experimental model, the DAMPs released are not encapsulated with lipids in contrast to other models (Collett et al., 2018). In a recent study on the secretion of intracellular components, it was found that many intracellular proteins and enzymes are secreted in an amphisome-dependent manner including cytosolic enzymes and nucleic acids (Jeppesen et al., 2019). The non-vesicular amphisome-secreted fraction isolated in this study has a protein composition remarkably similar to that observed in our study (**Figures 1, 2**). Thus, we conclude that a similar mechanism mediates the release of intracellular components as DAMPs during ER stress. Future work will examine mechanistically whether TG-induced release of DAMPs requires amphisome formation and fusion with the plasma membrane. A limitation of this study is the use of a single cell type (HepG2 cells) as a proxy for DAMP release from hepatocytes or other cell types which are known to undergo “chronic” ER stress *in vivo*. It will be critically important in future studies to extend these findings to other cell types *in vitro* and correlate the findings with *in vivo* models of chronic ER stress.

Many studies have demonstrated the link between ER stress and the production of DAMPs. Cellular stress induced by chemotherapeutics cause the release of DAMPs and so-called “immunogenic cell death” or ICD (van Vliet et al., 2015; Rufo et al., 2017). How ER stress couples to the release of DAMPs is still unknown, however, it is thought to require cell membrane permeabilization. We found robust production of DAMPs which could be purified in biochemically characterizable amounts in cells stressed with low doses of TG. Under these conditions we found minimal caspase activation and cell permeabilization. Thus, we conclude there is active release/secretion of DAMPs during chronic ER stress. It is well established that ER stress activates autophagic pathways to rid the cell of excess unfolded/misfolded polypeptide chains (Yorimitsu et al., 2006; Rashid et al., 2015; Cai et al., 2016). We propose a similar model wherein chronic ER stress leads to activation of autophagic pathways to rid the cell of misfolded proteins. Autophagic vesicles then form amphisomes which fuse with the plasma membrane to release the excess of misfolded proteins in an effort to restore proteostasis. This is consistent with other recent studies showing the release/secretion of misfolded proteins in chronically stressed cells *in vitro* and *in vivo* (Lim and Yue, 2015; Melentijevic et al., 2017). The released proteins then activate immune responses as DAMPs.

We have previously shown that burn injury leads to chronic systemic ER stress in multiple tissues, and in particular the liver (Gauglitz et al., 2009, 2010; Jeschke et al., 2009, 2012; Song et al., 2009; Jeschke and Boehning, 2012; Diao et al., 2014). This contributes to metabolic syndrome leading to adverse outcomes. In addition, burn injury leads to persistent systemic inflammation (Jeschke et al., 2004, 2007, 2011, 2012; Gauglitz et al., 2008; Jeschke, 2009; Stanojic et al., 2014) which may be linked to our finding in this study that ER stressed cells can be a potent source of DAMPs. In support of this link, clinical interventions that reduce ER stress such as tight control of blood glucose improves metabolic and inflammatory outcomes after burn injury (Jeschke and Boehning, 2012; Stanojic et al., 2018). The release of large amounts of intracellular antigens that we identified in this study may also induce autoimmune responses *in vivo*. Indeed, burn injury is known to exasperate autoimmune disease, at least in animal models (Anam et al., 2009). Future work will be necessary to evaluate the role of ER stress-associated DAMPs in the inflammatory response to thermal injury *in vivo*. Mechanistically, burn injury leads to calcium store depletion *via* IP₃R calcium channels leading to ER calcium store depletion and chronic hepatic ER stress (Jeschke et al., 2009). The IP₃R channel is a well-known central regulator of both ER stress and autophagic pathways (Jeschke and Boehning, 2011; Filippi-Chiela et al., 2016). Thus, the IP₃R calcium channel may provide the molecular link between burn injury, ER stress, and amphisome-mediated release of DAMPs. Future work will examine whether targeting this calcium channel is a potential therapeutic target to limit systemic inflammation and metabolic syndrome after a severe burn injury.

MATERIALS AND METHODS

Animals

This study was carried out in accordance with the recommendations of the National Institutes of Health Guidelines for the Use of Laboratory Animals. The protocol was approved by the Animal Care and Use Committee of the University of Texas Health Science Center. Female C57BL/6 mice were bred at the animal facility at the University of Texas and used at the age of 8–12 weeks.

Cell Culture and Treatment

HepG2 cells were purchased from ATCC and maintained in DMEM supplemented with 10% FBS, 1% penicillin/streptomycin, and 1% L-Glutamine. The cells were incubated at a constant temperature of 37°C and 5% CO₂. When the cells had grown to 80–90% confluency, thapsigargin (TG) purchased from Sigma-Aldrich was added to fresh media at a final concentration indicated in the text/figures. Thapsigargin added at 100 nM and 1 μM for 24 h produced similar amounts of NV DAMPs. Only DAMPs produced with 100 nM TG were used for biochemical characterization (Figures 4D–F) and DAMP functional analysis (Figures 4, 5). An equal volume of DMSO was used as a control condition. A typical DAMP preparation required starting material from 60 mls media isolated from 2 × 150 mm plates for each condition. This led to an average yield of approximately 50 μg protein at a concentration of 0.5 mg/ml.

Antibodies

Antibodies for Western blotting were purchased from the following sources: Histone H2A (Cell Signaling Technology #3636); HMGB1 (Cell Signaling Technology #6893); β-Actin (Cell Signaling Technology #3700); Profilin-1 (Cell Signaling Technology #3237); Enolase-1 (Cell Signaling Technology #3810); Bip/GRP78 (Cell Signaling Technology #3177); Alpha-fodrin (EMD Millipore #MAB1622); MLKL (Cell Signaling Technology #14993); Phospho-MLKL Ser358 (Cell Signaling Technology #91689); GAPDH (ThermoFisher #AM4300). Antibodies for flow cytometry were purchased from the following sources: F4/80, PE-Cyanine5 (ThermoFisher #15-4801-82); CD11b APC-eFluor 780 (ThermoFisher #47-0112-82); CD11c Alexa Fluor 700 (ThermoFisher #56-0114-82); CD86 (B7-2) FITC (ThermoFisher #11-0862-82); CD40 Super Bright 436 (ThermoFisher #62-0401-82); MHC Class II I-Ab (ThermoFisher #17-5320-82); CD25 Alexa Fluor 488 (ThermoFisher #53-0251-82); CD69 Alexa Fluor 700 (BioLegend #104539).

DAMP Isolation

The media collected from TG and DMSO treated cells were spun down at 1000 *xg* to remove dead cells and debris. The supernatants from this spin were transferred to round-bottomed centrifuge tubes and spun down at 40,000 *xg* at 4°C for 2 h using an SS-34 rotor in a super-centrifuge. The pellets from the 40,000 *xg* spin were resuspended in an equal volume of

PBS and 10 μL of each condition was removed for analysis by SDS-PAGE. The remainder of the resuspended pellets was diluted into PBS for density-gradient centrifugation. A 4 ml sucrose cushion consisting of 1 M sucrose and 0.2 M Tris base, pH 7.4 was transferred to centrifuge tubes and the resuspended pellets were carefully layered on top. The samples were placed in a Beckman SW-28 rotor and centrifuged at 100,000 g at 4°C for 75 min in an ultracentrifuge. The pellets from this final centrifugation were resuspended in TTB buffer (120 mM KCl, 50 mM Tris/HCl pH 8.0, 1 mM EDTA, 1 mM DTT, 1% Triton-X100) or PBS and passed through a 255/8 gauge needle before 10 μL of each condition was removed for analysis by SDS-PAGE.

Proteomic Analysis

Protein bands on Coomassie-stained SDS-PAGE gels were excised with a razor and subjected to mass spectrometry-based protein identification by the Clinical and Translational Proteomics Service Center, The Brown Foundation Institute of Molecular Medicine, The University of Texas Health Science Center at Houston. The gel band samples were subjected to in-gel digestion (Shevchenko et al., 2001). An aliquot of the tryptic digest (in 2% acetonitrile/0.1% formic acid in water) was analyzed by LC/MS/MS on an Orbitrap Fusion™ Tribrid™ mass spectrometer (Thermo Scientific™) interfaced with a Dionex UltiMate 3000 Binary RSLCnano System. Peptides were separated onto a Acclaim™ PepMap™ C18 column (75 μm ID \times 15 cm, 2 μm) at flow rate of 300 nl/min. Gradient conditions were: 3–22% solvent B (0.1% formic acid in acetonitrile) for 40 min; 22–35% B for 10 min; 35–90% B for 10 min; 90% B held for 10 min. The peptides were analyzed using data-dependent acquisition method, Orbitrap Fusion was operated with measurement of FTMS1 at resolutions 120,000 FWHM, scan range 350–1500 m/z , AGC target 2E5, and maximum injection time of 50 ms. During a maximum 3 s cycle time, the ITMS2 spectra were collected at rapid scan rate mode, with CID NCE 35, 1.6 m/z isolation window, AGC target 1E4, maximum injection time of 35 ms, and dynamic exclusion was employed for 35 s. The raw data files were processed using Thermo Scientific™ Proteome Discoverer™ software version 1.4. Spectra were searched against the IPI-Human database using the Sequest search engine run on an in-house server. Search results were trimmed to a 1% FDR for strict and 5% for relaxed condition using Percolator. Up to two missed cleavages were allowed. MS tolerance was set 10 ppm; MS/MS tolerance 0.8 Da. Carbamidomethylation on cysteine residues was used as fixed modification; oxidation of methionine as well as phosphorylation of serine, threonine and tyrosine were set as variable modifications.

Protease Sensitivity Assays to Assess Aggregation

Untreated HepG2 cells were cultured for 48 h, rinsed with PBS, and lysed with TTB buffer. The whole cell lysate was then diluted to the concentration of the DAMP isolation so that equivalent levels of protein were used. The whole cell lysate and DAMP

isolation were then exposed to a trypsin solution (10 $\mu\text{g}/\text{mL}$ trypsin, 30 $\mu\text{g}/\text{mL}$ chymostatin, 100 $\mu\text{g}/\text{mL}$ tosyl phenylalanyl chloromethyl ketone) in TTB for 0, 15, 30, 60, 120, and 180 min at 37°C. At the end of the exposure time, the samples were quenched and run on separate gradient gels for each condition and Coomassie stained.

Propidium Iodide Staining

HepG2 cells were removed from the plate after treatment and resuspended in propidium iodide and incubated in the dark for 15 min. The cells were then pelleted and resuspended in a small volume (\sim 10 μl) of PBS for plating on a glass slide with a coverslip. Brightfield and fluorescent images from at least five different fields for each slide were taken with a fluorescence microscope in a blinded manner. Each slide was quantified as the percentage of PI positive cells by a single blinded investigator (AA). The data in **Figure 3E** was pooled from three separate experimental replicates. The blind was broken at the end of the data collection. The images in **Supplementary Figure S3** are taken from the representative microscopic images used for analysis.

In vitro Generation of DCs and DC-Naïve CD4 + T Cell Co-culture

Dendritic cells were generated *in vitro* as previously described (Almanza et al., 2019). Briefly, tibias and femurs of C57BL/6 mice were removed under sterile conditions. Both ends of the bone were cut off, and the needle of a 1-mL syringe was inserted into the bone cavity to rinse the bone marrow out of the cavity. The cells were resuspended with Tris-NH₄Cl red blood cell lysis buffer to remove the red blood cells. Bone marrow cells were then cultured in DMEM with 10% FBS, glutamine, non-essential amino acids, sodium pyruvate, HEPES, and penicillin/streptomycin (complete medium) for 2 h. Floating cells were discarded and adherent cells were kept in complete medium with granulocyte-macrophage colony-stimulating factor (GM-CSF) (20 ng/ml) for 5 days. Complete medium and GM-CSF were renewed every 2 days. Immature DCs were treated with different concentration of DAMPs for 2 days and the supernatant was collected for cytokines analysis. In some experiments, stimulated DCs were processed for flow cytometry. Alternatively, stimulated DCs were re-plated in 96-well flat-bottom plates alone (3 \times 10⁵ cells/0.2 ml well volume) or with autologous naïve CD4+ T cells at a ratio of 1:10 for 5 days. Naïve CD4+ T cells were collected from the spleen and lymph nodes of WT mice using naïve CD4+ T cell isolation kit (Miltenyi Biotech). Co-culture supernatant was collected for cytokine analysis at the end of day 5.

Carboxyfluorescein Succinimidyl Ester (CFSE) Analysis

T cells were harvested and resuspended at 1 million cells per ml in PBS. CFSE (ThermoFisher C34554) was added to a final concentration of 1.5 μM and LIVE/DEAD™ Fixable Aqua Dead Cell Stain Kit (ThermoFisher #L34957) to a final concentration of 1 μM . Samples were vortexed gently and

let sit for 8 min at room temperature. An equal volume of pre-warmed FBS (100%, filtered) was then added. Cells were incubated at room temperature for 10 min. Cells were centrifuged for 5 min at 400 *xg*. Supernatants were discarded and the pellet vortexed to obtain a single cell suspension. Cells were washed again using PBS and fixed in 2% paraformaldehyde. Cells were stained at d0 with only CFSE before co-culture and harvested to be stained with live/dead aqua stain kit every 24 h for 4 continuous days. All cell analysis was conducted using a Beckman Coulter Gallios Flow Cytometer (BD Biosciences, San Jose, CA, United States) and data were analyzed by Kaluza Analysis Software. Results were shown as a representative of two independent experiments.

Assessment of the Cytokine Profile

Concentrations of IFN- γ , IL-13, IL-6, IL-17 (R&D Systems), and TNF- α (Thermo Fisher) in DCs or DC/T-cell co-culture supernatants were measured by ELISA, according to the manufacturer's recommendations, and expressed in picograms per milliliter. Results were expressed as mean \pm standard deviation.

Phenotype Analysis

DC phenotype was evaluated by flow cytometry using a standardized protocol (Sovolyova et al., 2014). Cells were kept on ice during all the procedures. For the extracellular markers, cells were stained with CD11c-AF700, F4/80-PE-Cy5, CD11b-APC-eF780, MHCII (I-Ab)-APC, CD40-Ef450, and CD86-FITC (see section "Antibodies"). Detection of cell surface markers was conducted using a Beckman-Coulter Gallios Flow Cytometer (BD Biosciences, San Jose, CA, United States) and data were analyzed by Kaluza Analysis Software. Live/dead assays were determined using the Aqua Dead Cell Stain Kit (ThermoFisher #L34957). Results were shown as mean \pm standard deviation.

REFERENCES

- Alicka, M., and Marycz, K. (2018). The effect of chronic inflammation and oxidative and endoplasmic reticulum stress in the course of metabolic syndrome and its therapy. *Stem. Cells Int.* 2018, 4274361. doi: 10.1155/2018/4274361
- Almanza, A., Carlesso, A., Chintha, C., Creedican, S., Doultinos, D., and Leuzzi, B. (2019). Endoplasmic reticulum stress signalling - from basic mechanisms to clinical applications. *FEBS J.* 286, 241–278. doi: 10.1111/febs.14608
- Anam, K., Amare, M., Naik, S., Szabo, K. A., and Davis, T. A. (2009). Severe tissue trauma triggers the autoimmune state systemic lupus erythematosus in the MRL/++ lupus-prone mouse. *Lupus* 18, 318–331. doi: 10.1177/0961203308097479
- Bradford, M. M. (1976). A rapid and sensitive method for the quantitation of microgram quantities of protein utilizing the principle of protein-dye binding. *Anal. Biochem.* 72, 248–254. doi: 10.1006/abio.1976.9999
- Brooks, N. C., Marshall, A. H., Qa'aty, N., Hiyama, Y., Boehning, D., and Jeschke, M. G. (2013). XBP-1s is linked to suppressed gluconeogenesis in the ebb phase of burn injury. *Mol. Med.* 19, 72–78. doi: 10.2119/molmed.2012.00348

DATA AVAILABILITY

The datasets generated for this study are available on request to the corresponding authors.

ETHICS STATEMENT

The animal study was reviewed and approved by Animal Care and Use Committee of The University of Texas Health Science Center at Houston.

AUTHOR CONTRIBUTIONS

AIA, MG, YF, MT, and AbA performed the experiments. AIA, MG, YF, MT, AMA, AbA, MJ, and DB analyzed the data and prepared the figures. MJ and DB conceived the project. All authors contributed intellectually, wrote, and approved the final manuscript.

FUNDING

This work was supported by the National Institute of Health grants R01GM081685 (DB), R01GM087285 (MJ, DB), and R01GM115446 (AMA). The proteomic studies were supported in part by the Clinical and Translational Proteomics Service Center at The University of Texas Health Science Center at Houston.

SUPPLEMENTARY MATERIAL

The Supplementary Material for this article can be found online at: <https://www.frontiersin.org/articles/10.3389/fcell.2019.00198/full#supplementary-material>

- Cai, Y., Arikath, J., Yang, L., Guo, M. L., Periyasamy, P., and Buch, S. (2016). Interplay of endoplasmic reticulum stress and autophagy in neurodegenerative disorders. *Autophagy* 12, 225–244. doi: 10.1080/15548627.2015.1121360
- Carta, S., Semino, C., Sitia, R., and Rubartelli, A. (2017). Dysregulated IL-1beta secretion in autoinflammatory diseases: a matter of stress? *Front. Immunol.* 8:345. doi: 10.3389/fimmu.2017.00345
- Caruso, S., and Poon, I. K. H. (2018). Apoptotic cell-derived extracellular vesicles: more than just debris. *Front. Immunol.* 9:1486. doi: 10.3389/fimmu.2018.01486
- Choi, A. M., and Nakahira, K. (2011). Dampening insulin signaling by an NLRP3 'meta-flammasome'. *Nat. Immunol.* 12, 379–380. doi: 10.1038/ni.2028
- Collett, G. P., Redman, C. W., Sargent, I. L., and Vatish, M. (2018). Endoplasmic reticulum stress stimulates the release of extracellular vesicles carrying danger-associated molecular pattern (DAMP) molecules. *Oncotarget* 9, 6707–6717. doi: 10.18632/oncotarget.24158
- Davis, B. K., Wen, H., and Ting, J. P. (2011). The inflammasome NLRs in immunity, inflammation, and associated diseases. *Annu. Rev. Immunol.* 29, 707–735. doi: 10.1146/annurev-immunol-031210-101405
- Diao, L., Marshall, A. H., Dai, X., Bogdanovic, E., Abdullahi, A., Amini-Nik, S., et al. (2014). Burn plus lipopolysaccharide augments endoplasmic reticulum stress and NLRP3 inflammasome activation and reduces PGC-1alpha in liver. *Shock* 41, 138–144. doi: 10.1097/SHK.0000000000000075

- Fang, H., Ang, B., Xu, X., Huang, X., Wu, Y., Sun, Y., et al. (2014). TLR4 is essential for dendritic cell activation and anti-tumor T-cell response enhancement by DAMPs released from chemically stressed cancer cells. *Cell Mol. Immunol.* 11, 150–159. doi: 10.1038/cmi.2013.59
- Faruqi, F. N., Xu, L., and Al-Jamal, K. T. (2018). Preparation of exosomes for siRNA delivery to cancer cells. *J. Vis. Exp.* 142, e58814. doi: 10.3791/58814
- Filippi-Chiela, E. C., Viegas, M. S., Thome, M. P., Buffon, A., Wink, M. R., and Lenz, G. (2016). Modulation of autophagy by calcium signalosome in human disease. *Mol. Pharmacol.* 90, 371–384. doi: 10.1124/mol.116.105171
- Gauglitz, G. G., Halder, S., Boehning, D. F., Kulp, G. A., Herndon, D. N., Barral, J. M., et al. (2009). Post-burn hepatic insulin resistance is associated with er stress. *Shock* 33, 299–305. doi: 10.1097/SHK.0b013e3181b2f439
- Gauglitz, G. G., Halder, S., Boehning, D. F., Kulp, G. A., Herndon, D. N., Barral, J. M., et al. (2010). Post-burn hepatic insulin resistance is associated with endoplasmic reticulum (ER) stress. *Shock* 33, 299–305. doi: 10.1097/SHK.0b013e3181b2f439
- Gauglitz, G. G., Song, J., Herndon, D. N., Finnerty, C. C., Boehning, D., Barral, J. M., et al. (2008). Characterization of the inflammatory response during acute and post-acute phases after severe burn. *Shock* 30, 503–507. doi: 10.1097/SHK.0b013e31816e3373
- Gupta, S., Rawat, S., Arora, V., Kottarath, S. K., Dinda, A. K., Vaishnav, P. K., et al. (2018). An improvised one-step sucrose cushion ultracentrifugation method for exosome isolation from culture supernatants of mesenchymal stem cells. *Stem. Cell. Res. Ther.* 9:180. doi: 10.1186/s13287-018-0923-0
- He, Y., Hara, H., and Nunez, G. (2016). Mechanism and regulation of NLRP3 inflammasome activation. *Trends Biochem. Sci.* 41, 1012–1021. doi: 10.1016/j.tibs.2016.09.002
- Hotamisligil, G. S. (2010). Endoplasmic reticulum stress and the inflammatory basis of metabolic disease. *Cell* 140, 900–917. doi: 10.1016/j.cell.2010.02.034
- Jeppesen, D. K., Fenix, A. M., Franklin, J. L., Higginbotham, J. N., Zhang, Q., Zimmerman, L. J., et al. (2019). Reassessment of exosome composition. *Cell* 177, 428–445.e18. doi: 10.1016/j.cell.2019.02.029
- Jeschke, M. G. (2009). The hepatic response to thermal injury: is the liver important for postburn outcomes? *Mol. Med.* 15, 337–351. doi: 10.2119/molmed.2009.00005
- Jeschke, M. G., Barrow, R. E., and Herndon, D. N. (2004). Extended hypermetabolic response of the liver in severely burned pediatric patients. *Arch. Surg.* 139, 641–647.
- Jeschke, M. G., and Boehning, D. (2011). Endoplasmic reticulum stress and insulin resistance post-trauma: similarities to type 2 diabetes. *J. Cell. Mol. Med.* 16, 437–444. doi: 10.1111/j.1582-4934.2011.01405.x
- Jeschke, M. G., and Boehning, D. (2012). Endoplasmic reticulum stress and insulin resistance post-trauma: similarities to type 2 diabetes. *J. Cell Mol. Med.* 16, 437–444. doi: 10.1111/j.1582-4934.2011.01405.x
- Jeschke, M. G., Boehning, D. F., Finnerty, C. C., and Herndon, D. N. (2007). Effect of insulin on the inflammatory and acute phase response after burn injury. *Crit. Care Med.* 35, S519–S523.
- Jeschke, M. G., Finnerty, C. C., Herndon, D. N., Song, J., Boehning, D., Tompkins, R. G., et al. (2012). Severe injury is associated with insulin resistance, endoplasmic reticulum stress response, and unfolded protein response. *Ann. Surg.* 255, 370–378. doi: 10.1097/SLA.0b013e31823e76e7
- Jeschke, M. G., Gauglitz, G. G., Kulp, G. A., Finnerty, C. C., Williams, F. N., Kraft, R., et al. (2011). Long-term persistence of the pathophysiological response to severe burn injury. *PLoS One* 6:e21245. doi: 10.1371/journal.pone.0021245
- Jeschke, M. G., Gauglitz, G. G., Song, J., Kulp, G. A., Finnerty, C. C., Cox, R. A., et al. (2009). Calcium and ER stress mediate hepatic apoptosis after burn injury. *J. Cell Mol. Med.* 13, 1857–1865. doi: 10.1111/j.1582-4934.2009.00644.x
- Jo, E. K., Kim, J. K., Shin, D. M., and Sasakawa, C. (2016). Molecular mechanisms regulating NLRP3 inflammasome activation. *Cell. Mol. Immunol.* 13, 148–159. doi: 10.1038/cmi.2015.95
- Konoshenko, M. Y., Lekchnov, E. A., Vlassov, A. V., and Laktionov, P. P. (2018). Isolation of extracellular vesicles: general methodologies and latest trends. *Biomed. Res. Int.* 2018:8545347. doi: 10.1155/2018/8545347
- Lim, J., and Yue, Z. (2015). Neuronal aggregates: formation, clearance, and spreading. *Dev. Cell* 32, 491–501. doi: 10.1016/j.devcel.2015.02.002
- Liu, Z., Zhao, N., Zhu, H., Zhu, S., Pan, S., Xu, J., et al. (2015). Circulating interleukin-1beta promotes endoplasmic reticulum stress-induced myocytes apoptosis in diabetic cardiomyopathy via interleukin-1 receptor-associated kinase-2. *Cardiovasc. Diabetol.* 14:125. doi: 10.1186/s12933-015-0288-y
- Melentjevic, I., Toth, M. L., Arnold, M. L., Guasp, R. J., Harinath, G., and Nguyen, K. C. (2017). C. elegans neurons jettison protein aggregates and mitochondria under neurotoxic stress. *Nature* 542, 367–371. doi: 10.1038/nature21362
- Oakes, S. A., and Papa, F. R. (2015). The role of endoplasmic reticulum stress in human pathology. *Annu. Rev. Pathol.* 10, 173–194. doi: 10.1146/annurev-pathol-012513-104649
- O'Neill, C. M., Lu, C., Corbin, K. L., Sharma, P. R., Dula, S. B., Carter, J. D., et al. (2013). Circulating levels of IL-1B+IL-6 cause ER stress and dysfunction in islets from prediabetic male mice. *Endocrinology* 154, 3077–3088. doi: 10.1210/en.2012-2138
- Qiu, G. H., Xie, X., Xu, F., Shi, X., Wang, Y., and Deng, L. (2015). Distinctive pharmacological differences between liver cancer cell lines HepG2 and Hep3B. *Cytotechnology* 67, 1–12. doi: 10.1007/s10616-014-9761-9
- Rani, M., Nicholson, S. E., Zhang, Q., and Schwacha, M. G. (2017). Damage-associated molecular patterns (DAMPs) released after burn are associated with inflammation and monocyte activation. *Burns* 43, 297–303. doi: 10.1016/j.burns.2016.10.001
- Rashid, H. O., Yadav, R. K., Kim, H. R., and Chae, H. J. (2015). ER stress: autophagy induction, inhibition and selection. *Autophagy* 11, 1956–1977. doi: 10.1080/15548627.2015.1091141
- Rufo, N., Garg, A. D., and Agostinis, P. (2017). The unfolded protein response in immunogenic cell death and cancer immunotherapy. *Trends Cancer* 3, 643–658. doi: 10.1016/j.trecan.2017.07.002
- Sano, R., and Reed, J. C. (2013). ER stress-induced cell death mechanisms. *Biochim. Biophys. Acta* 1833, 3460–3470. doi: 10.1016/j.bbamer.2013.06.028
- Shevchenko, A., Loboda, A., Ens, W., Schraven, B., Standing, K. G., and Shevchenko, A. (2001). Archived polyacrylamide gels as a resource for proteome characterization by mass spectrometry. *Electrophoresis* 22, 1194–1203. doi: 10.1002/1522-2683(22)6<1194::aid-elps1194>3.0.co;2-a
- Slany, A., Haudek, V. J., Zwickl, H., Gundacker, N. C., Grusch, M., Weiss, T. S., et al. (2010). Cell characterization by proteome profiling applied to primary hepatocytes and hepatocyte cell lines Hep-G2 and Hep-3B. *J. Proteome Res.* 9, 6–21. doi: 10.1021/pr900057t
- Song, J., Finnerty, C. C., Herndon, D. N., Boehning, D., and Jeschke, M. G. (2009). Severe burn-induced endoplasmic reticulum stress and hepatic damage in mice. *Mol. Med.* 15, 316–320. doi: 10.2119/molmed.2009.00048
- Song, J., Zhang, X. J., Boehning, D., Brooks, N. C., Herndon, D. N., and Jeschke, M. G. (2012). Measurement of hepatic protein fractional synthetic rate with stable isotope labeling technique in thapsigargin stressed HepG2 cells. *Int. J. Biol. Sci.* 8, 265–271. doi: 10.7150/ijbs.3660
- Sovolyova, N., Healy, S., Samali, A., and Logue, S. E. (2014). Stressed to death - mechanisms of ER stress-induced cell death. *Biol. Chem.* 395, 1–13. doi: 10.1515/hsz-2013-0174
- Stanojic, M., Abdullahi, A., Rehoh, S., Parousis, A., and Jeschke, M. G. (2018). pathophysiological response to burn injury in adults. *Ann. Surg.* 267, 576–584. doi: 10.1097/SLA.0000000000002097
- Stanojic, M., Chen, P., Harrison, R. A., Wang, V., Antonyshyn, J., Zuniga-Pflucker, J. C., et al. (2014). Leukocyte infiltration and activation of the NLRP3 inflammasome in white adipose tissue following thermal injury. *Crit. Care Med.* 42, 1357–1364. doi: 10.1097/CCM.0000000000000209
- Tang, D., Kang, R., Coyne, C. B., Zeh, H. J., and Lotze, M. T. (2012). PAMPs and DAMPs: signal 0s that spur autophagy and immunity. *Immunol. Rev.* 249, 158–175. doi: 10.1111/j.1600-065X.2012.01146.x
- van Vliet, A. R., Martin, S., Garg, A. D., and Agostinis, P. (2015). The PERKs of damage-associated molecular patterns mediating cancer immunogenicity: from sensor to the plasma membrane and beyond. *Semin Cancer Biol.* 33, 74–85. doi: 10.1016/j.semcancer.2015.03.010
- Vinaik, R., Stanojic, M., and Jeschke, M. G. (2018). NLRP3 inflammasome modulates post-burn lipolysis and hepatic fat infiltration via fatty acid synthase. *Sci. Rep.* 8:15197. doi: 10.1038/s41598-018-33486-9

- Wang, W., Li, J., Wu, K., Azhati, B., and Rexiati, M. (2016). Culture and identification of mouse bone marrow-derived dendritic cells and their capability to induce T lymphocyte proliferation. *Med. Sci. Monit.* 22, 244–250. doi: 10.12659/msm.896951
- Yorimitsu, T., Nair, U., Yang, Z., and Klionsky, D. J. (2006). Endoplasmic reticulum stress triggers autophagy. *J. Biol. Chem.* 281, 30299–30304. doi: 10.1074/jbc.m607007200
- Zhang, K., Shen, X., Wu, J., Sakaki, K., Saunders, T., Rutkowski, D. T., et al. (2006). Endoplasmic reticulum stress activates cleavage of CREBH to induce a systemic inflammatory response. *Cell* 124, 587–599. doi: 10.1016/j.cell.2005.11.040

Conflict of Interest Statement: The authors declare that the research was conducted in the absence of any commercial or financial relationships that could be construed as a potential conflict of interest.

Copyright © 2019 Andersohn, Garcia, Fan, Thompson, Akimzhanov, Abdullahi, Jeschke and Boehning. This is an open-access article distributed under the terms of the Creative Commons Attribution License (CC BY). The use, distribution or reproduction in other forums is permitted, provided the original author(s) and the copyright owner(s) are credited and that the original publication in this journal is cited, in accordance with accepted academic practice. No use, distribution or reproduction is permitted which does not comply with these terms.